A STEP-BY-STEP PROCEDURE FOR DETERMINING THERMAL RESISTIVITY COEFFICIENTS OF DOPED POLYSILICON THIN FILMS

利用一實驗程序來決定多晶矽薄膜之電阻溫度係數

Chi Hsiang Pan 潘吉祥
Department of Mechanical Engineering in National Chin-Yi Institute of Technology, Taichung, Taiwan, ROC
E-mail: pancs@chinyi.ncit.edu.tw,
Phone: 886-4-23924505 ext 7155,
Fax: 886-4-23930681

ABSTRACT

We propose a step-by-step procedure to experimentally determine thermal resistivity coefficients (TRC) of doped polysilicon thin films using micromachined test structures and common experimental apparatus. The test structures can be fabricated by simple silicon-based micromachining techniques and in-situ along with the active devices on the same chip for monitoring the TRC of thin films. Besides, they occupy a very small area on a MEMS die site. The experimental apparatus include a conventional electronics probe station equipped with a CCD, an image analysis system, I-V power supply and a temperature controlled heating stage, which are available in electronic or IC laboratory. Unlike traditional methods, the resistivity-temperature (ρ-T) characteristic is established through the displacement and I-V measurements of test structures, and the temperatures of test structures are determined by using a temperature-controlled heating stage. Based on feasible assumptions, the experimental procedures and apparatus for determining R-T characteristics are quit simple than conventional methods. Phosphorous-doped LPCVD polysilicon films are used herein to demonstrate the effectiveness of the proposed method, while the method is also applicable to other conducting films. The TRC of phosphorous-doped LPCVD polysilicon films is about 2.3×10^{-3}℃$^{-1}$ from room temperature to 900℃.

摘要

本文利用微加工測試結構和一般實驗儀器，並提出一實驗步驟程序來決定多晶矽薄膜之電阻溫度係數。測試結構可利用簡單矽微加工技術製作，而且可同時與元件製作在相同晶片上，以檢測薄膜的電阻溫度係數。測試結構僅佔晶片非常微小的區域。實驗所用的儀器包括裝設有 CCD 之傳統電子探針台、影像擷取處理系統、I-V 供應器以及溫控台，這些在一般電子或 IC 廠可方便取得。不像傳統的方法，本文是透過量測測試結構位移及 I-V 圖來建構電阻-溫度之間的特性，而測試結構之溫度是由溫控台來決定。因此在實驗儀器及步驟程序上都比傳統方法簡單。本文以參磷之多晶矽薄膜來驗證本方法之效益性，然而此方法是可以應用在其他的導電薄膜材料上。由實驗量得在室溫至 900℃之間，參磷之多晶矽薄膜的電阻溫度係數約爲 2.3×10^{-3}℃$^{-1}$

1. INTRODUCTION

MEMS devices are of great interest for a variety of applications in science and technology. The principles of resistive (or joule-) heating-induced thermo-mechanical effects, for instance thermal expansion and bimorph effect, have been widely used as actuation mechanisms for micro actuators in MEMS, such as bimetal [1], bi-stable [2], buckling [3,4], thermo-magnetic [5], and other electro-thermal [6,7]. Resistive-heating effect is also conventionally applied to sensing in micro thermal sensors [8,9] and in the measurement of thermal-physical properties of thin films [10,11]. In addition, thermal micro-assembly techniques [12], thermal-plastic reshaping technologies [13], and re-crystallization of amorphous films [14] using resistive-heating effect are reported. Commonly, doped LPCVD polycrystalline silicon films are the fundamental materials to form the resistive heating layer. Therefore, the resistivity of doped polysilicon thin film is expected to play an essential role for the development of MEMS devices that are based on the resistive-heating effect. Basically, the resistivity of doped thin films is process dependent, impurity concentration dependent and temperature dependent. Unfortunately, the database for such property with respect to these parameters has not been fully established. Therefore, the convenient and accurate determination of resistivity-temperature (ρ-T) characteristic, i.e. the measurement of thermal resistivity coefficient (TRC), is highly desirable to guarantee the design of electro-thermal MEMS devices.

Traditionally, TRC is determined by good curve fitting agreement between the electro-thermal theoretical curve and I-V measured data. Oil-bath method [15] is one of the commonly used techniques. In this method, the I-V characteristics of the test structures are measured using a semiconductor parameter analyzer (such as HP4145B) under two conditions: (1) with the test structures placed in a high vacuum, (2) with the packages, containing the test structures, filled with electrically insulating silicon oil. The oil acts as a heat exchanger, holding the test structure at a series of temperature values T_{oil}, which is adjusted by a hot chuck used as an external heat source in contact with the packages. The temperature (T_{oil}) of the silicon oil is measured by a thermocouple attached to the packages. Since the temperatures of test structures are the same at each of the intercepts of the I-V characteristics under (1) and (2) conditions, therefore, the R-T characteristics of test structures under condition (1) are obtained. In this method, in order to avoid the Joule-heating of the test structures to affect the oil temperature of the system, small currents are applied to the test structures. Anyway, the temperature of test structures are somewhat greater than the oil temperature, thus the difference must be accounted. Another feasible approach [16] to determine TRC is to measure the I-V characteristics of the test structures in high vacuum conditions and to derive the temperatures of test structures from the steady-state heat equation. Thereby, TRC can be determined by good curve fitting agreement between the resistance equation (derived from the heat equation) and I-V measured data with TRC as the only one fitting parameter. In this approach, all other parameters such as thermal conductivity coefficient, sheet resistance and contact resistance are either known or measurable. To monitor the temperature, an approach [17] has been adopted by applying a heating resistor to elevate a temperature gradient at the test structure and by using polysilicon resistors as a resistance thermometer.

In this paper, we present a step-by-step procedure to experimentally determine TRC of doped polysilicon thin films using micromachined test structures and common experimental apparatus. The test structures can be fabricated by silicon-micromachining techniques (sacrificial-layer surface micromachining or post-bulk

micromachining technique) and in-situ along with the active devices on the same chip for monitoring TRC of the thin films. Besides, they occupy a very small area on a MEMS die site. The experimental apparatus include a conventional electronics probe station equipped with a CCD, an image analysis system, I-V power supply and a temperature controlled heating stage (hot chuck), which are available in electronic or IC laboratory. Unlike traditional methods, the R-T characteristic is established through the displacement and I-V measurements of test structures, and the temperatures of test structures are determined by using a temperature-controlled heating stage. Phosphorous-doped LPCVD polysilicon films are used herein to demonstrate the effectiveness of the proposed method.

2. OPERATING PRINCIPLE

Figure 1 schematically depicts the micromachined test structure in this study, which is similar to the author's previous works [18,19]. The test structure consists of a pair of cantilever beams with different lengths connected by a short tip beam. Two cantilever beams are designed as test beams, and the tip beam acts as an indicator. As the temperature rises using a heating stage or applying current through the test structure (as shown in Fig. 2(a) and (b), respectively), the difference between the two test beams with respect to elongation causes the deflection of the two beams, thereby magnifying the lateral displacement of the tip. The elongation is due to thermally induced strain. Since the displacement of the tip beam is sufficiently large, direct observations under an optical microscope can be used to collect reasonably accurate data. A Vernier gauge located at free end of the indicator beam can be used to quantify the displacement, but this is optional.

3. TEST STRUCTURES FABRICATION

The test structures employed in measurement are made of LPCVD polycrystalline silicon films at 620℃ with a silane (SiH4) flow rate of 40 sccm, a pressure of 107 mtorr and deposition time of 260min., following a high temperature phosphorus-diffusion step ($POCL_3$) at 900℃ deposition about 40 minutes and with 1050℃ drive-in and annealing for 1 hour. The film thickness is about 2 μm, which is accurate to ±0.5%. PECVD TEOS SiO_2 with about thickness of 3 μm is used as sacrificial layer. A conventional surface-sacrificial layer or post-bulk micromachining techniques are used to fabricate the test structures, as shown in Fig. 3 and Fig. 4 respectively. Post-bulk micromachining is to etch a deeper cavity beneath the test structure, so that the thermal isolation between the test structure and the substrate can be enhanced. Figure 5 displays the SEM photographs of the test structures with different beam lengths. Figure 5(a) is the original design and (b) is a symmetric design with two pairs of the test structures so that a double displacement can be obtained by taking the difference of the distance between two tip beams.

4. EXPERIMENTS

The experimental apparatus, which consist of an optical microscope mounted with a CCD and two units placed under the microscope, are shown in Fig. 6. The CCD is connected with a computer that is installed with an

imaging software (Matrox Inspector version 3.1) for image capture, measuring, analysis and processing. The two units are a temperature-controlled heating stage and probe stages connected with a current/voltage adjustable power supply. The dimensions of the test structure demonstrated herein are: the lengths of long beams and short beams varying from 200 μm to 600 μm, the width is 3 μm, the thickness is 2 μm, and the gap distance between the central lines of two test beams equals 5 μm. All dimensions are with accuracy to $\pm 1\%$

Experimental procedures carried out to determine TRC are described as follow. In the first step, the heating stage is placed under the microscope to heat up the test structures. The displacement and temperature (δ–T) relationship can be obtained, as shown in Fig. 7. In order to prevent either creep or recrystallization [13], measurements are made on each sample in the temperature ranging from room temperature to 900℃. A Nitrogen-gas atmosphere prevents oxidation of the sample. In the second step, probe stages connected with an I/V adjustable power supply are placed under the microscope to apply current/voltage dissipating a heating power through the test structures. Firstly, voltages V are applied to the test structures, and the displacements δ are measured. Thereby, the displacement-voltage (δ-V) relationship and current-voltage (I-V) relationship can be obtained simultaneously. After that, relating the (δ-V) relationship to the (δ–T) relationship, the (V–T) diagram can be obtained, as shown in Fig. 8. According to the (I-V) relationship and the Ohmic principle R=V/I, the resistance-voltage (R–V) relationship (Fig. 9) is obtained, where R is total resistance of the measured system. After that, relating the (R-V) relationship with the (V-T) diagram, then finally, the (R-T) relationship is obtained. Since the total resistance R consists of the resistance of the test structure itself and the contact resistance, so it is required to know the contact resistance beforehand to measure exactly the resistivity of the thin film. The value of the contact resistance is obtained by plotting the measured resistances of test structures with different beam lengths, and extracting the intercept resistance corresponding to the length of zero, which is the contact resistance. Subtracting contact resistance from total resistance, the resistivity-temperature (ρ-T) characteristic of test structures is obtained, as shown in Fig. 10. The experimental apparatus and above procedures for determining ρ-T characteristics are simpler than conventional methods [15-17]. Suppose that the temperature dependent electrical resistivity $\rho(T)$ is with a linear temperature coefficient ε as follow [20]

$$\rho(T) = \rho_o \cdot (1 + \varepsilon \cdot (T - T_o)) \tag{1}$$

ρ_o is the electrical resistivity at room temperature T_0. Thus, using Eq. (1) to fit the ρ-T characteristics linearly with ε as the only fitting parameter and calculating the slope of the line, thereby, ε is obtained. From some sets of measurements, ε is about 2.3×10^{-3}℃$^{-1}$. Besides, the ρ_o value also be obtained and is around $2.5 \times 10^{-5}\,\Omega$-m. The difference in the values compared to other reports may result from different process conditions, impurity concentrations and grain size of thin films [3,15-17,21].

5. RESULTS AND DISCUSSIONS

According to Fig. 9 and Fig. 10, the resistance of test structure increases with the applied voltage since the doped polysilicon film has a positive TRC. In addition, the approximately linear temperature dependence of the resistivity is slightly non-linear at higher temperatures. Some potential factors to influence the uncertainty of results are considered as well. The first factor is dominated by the non-ideality of test beams such as side walls free from vertical. The detailed knowledge of the influence of cross section geometry is in reference [18]. The effect can be less than 1.5%. One solvable method to reduce the effect is using high anisotropic-RIE (Ion

Reactive Etching) to produce vertical side walls. The undercut of anchor under the contact pads due to isotropic etching of the sacrificial layer makes the boundary condition of anchors slightly different from ideal geometry also. Fortunately, this makes very little deviation in the displacement of test structure. The second factor is dominated by contribution from the pad resistance and the contact resistance between the probe and the pad. Both may influence the thermal response and I-V characteristics of the test structure. Since test beams are quite long and the pads are much larger than the beam width, It can be assumed that the pad resistance is much smaller than the resistance of test structure, therefore the temperature at pads can be essentially near the ambient temperature [12,15,21] and meanwhile the deviation of the thermal response of test structure can be neglect. The detailed discussion is in Appendix A. As for the floating contact resistance between the probe and the pad, this can be improved using aluminum metallization pads or bonding with wires. The third factor is that there is also a degree of uncertainty in the predicted heat losses from the test structure through the heat transfer conditions. According to the numerical estimation (see Appendix B), the conduction heat loss through air to the surrounding, convection heat loss and radiation heat loss in lower temperature are obviously negligible. However, the conduction heat loss through air to the substrate seems to be not neglected. It is obvious that conduction heat loss through air to the substrate is strongly governed by the temperature of test beams, the elevation of the test beam above the substrate and the thermal insulation of deposited layers on the substrate. Thus a deep trench etched under the test structure, and thick and low thermal conductive layers deposited on the substrate can increase the thermal isolation from the substrate, thereby increasing the accuracy of the original heat equation in the paper. Besides, lower operation temperature can also reduce substantial thermal radiation and heat conduction to the substrate. Therefore, for simplicity, the influence of the heat conduction through the air to the substrate is assumed ignored in the paper. Otherwise, if necessary, we can modify the test structure to be heated in high vacuum further. Thus, we can certainly assume that heat is transported only by conduction through the test beams to the contact pads (heat sinks) because the other heat losses are negligible [12,15,21,22]. The last factor is that a captured image photograph of a test structure under a bias processed in imaging software (Matrox Inspector version 3.1) to measure the lateral deflection has the uncertainty about ± 0.1 um is estimated from the clarity of the image, which may lead to source of discrepancy in obtaining TRC.

6. CONCLUSION

This work presents a simple method for determining TRC of thin films based on the behavior of test structures produced with the films. Compared to the previous reported methods, the proposed test structures are quiet compact and easily fabricated, and the experimental apparatus are available in a laboratory. In addition, based on feasible assumptions, the method has its own merits. (1) The temperature of Joule-heated test structure is determined by measuring the displacement of the test microstructure, and the displacement can be directly measured under an optical microscope equipped a CCD; (2) The resistivity-temperature ρ-T characteristic is obtained without using any semiconductor parameter analyzer. Experimental results with a phosphorous-doped LPCVD polycrystalline silicon film are used to demonstrate the effectiveness of the proposed method, while the method is also applicable to other conducting films. From some sets of measurements, the TRC of phosphorous-doped LPCVD polysilicon films is about 2.3×10^{-3}℃$^{-1}$ from room temperature to 900℃$^{-1}$.

ACKNOWLEDGMENTS

This work is supported by the National Science Council of the Republic of China under Contract No. NSC 91-2218-E-167-001. The staffs of the Semiconductor Research Center at National Chiao Tung University are also appreciated, along with Dr. R. H. Horng for providing experiments at NCHU.

Appendix A

The test beams conduct the heat to the anchor pads and since the anchor pads are not perfect conductors of the heat, therefore the anchor pads will heat up. The temperature at the anchor pads T_p can be given by an equation [12]

$$T_p=\{\Psi \bullet T_s/A_b+J\sqrt{\rho_o\kappa/\varepsilon} \bullet (1-\varepsilon T_o) \bullet \tan (J \bullet L/2 \bullet \sqrt{\rho_o\varepsilon})\}/\{\Psi/A_b-J\sqrt{\rho_o\kappa\varepsilon}\} \tag{A-1}$$

Symbol κ denotes the thermal conductivity coefficient of test films, ρ_o is the electrical resistivity at room temperature T_o, T_s is the substrate temperature, ε is the temperature coefficient of the resistivity, and J denotes the current density through the beams. A_b = hw is the cross section area of test beams and L is the total length of beams. $\Psi=\kappa_o/t_o$ is the effective thermal conductance (W/℃) of pads. t_o is the thickness of anchor, and κ_o is the thermal conductivity of anchor. The temperature at the pads in our test structures can be examined using the given example that L=600um, w=3um, h=2um, t_o=3um, To=T_s= 20℃, κ =39W/m℃, κ_o=1.4W/m℃, ρ_o =$2.5\times10^{-5}\Omega$-m, and $\varepsilon=2.3\times10^{-3}$℃$^{-1}$. The current density J is calculated by J=I/A_b. Evaluation of Eq. (A-1) gives $T_p\sim32$℃. Hence; we can conclude that the pad heating is not significant. Basically, for long test beams and large pads, the temperature at pads can be assumed essentially near the ambient temperature [12,15,21,22].

Appendix B

Under steady-state conditions, resistive heating power generated in the test structure flows out of the test structure by six ways: (1) conduction through the test beams to the substrate, (2) conduction through the air to surrounding, (3) conduction through the air to the substrate, (4) convection through the air, (5) radiation to the air, and (6) radiation to the substrate. The following show a numerical estimate.

(1) The heat conduction through the test beams to the substrate is approximate

$$Q_{conduction,\ polysi}= -\kappa_{polysi}(T-T_s)/L \tag{B-1}$$

Where T is the average temperature along the test structure and Ts is the temperature of substrate. κ_{polysi} denotes the conductive coefficient of test structure and L is the total length of test beams.

(2) The heat conduction through the air to surrounding is calculated in the same way as done by [15]

$$Q_{conduction,\ air}= -1/4 \bullet \eta\ \Lambda P(273.2/T_{\infty})^{1/2}(T-T_{\infty}) \tag{B-2}$$

Where η is the accommodation coefficient, Λ is the free-molecule heat conductivity at 273.2K, and T_{∞} is the ambient temperature.

(3) The heat conduction through the air to the substrate is approximately governed by

$$Q_{conduction,\ air,\ sub}= -S_c\kappa_{air}(T-T_s)/g_{air}= -S_c(T-T_s)/R_T \tag{B-3}$$

Where κ_{air} is the air conductive coefficient, and g_{air} is the gap distance between the test beams and the substrate. R_T denotes the thermal resistance between the test beams and the substrate, and is given by

$$R_T = g_{air}/\kappa_{air} \quad \text{(B-4)}$$

If the surface of substrate is deposited with other layers, such as silicon nitride and oxide, which can enhance thermal insulation, R_T is given by

$$R_T = g_{air}/\kappa_{air} + t_o/\kappa_o + t_n/\kappa_n \quad \text{(B-5)}$$

Where t_o and t_n are the thickness of Si_3N_4 and SiO_2, respectively and, κ_o and κ_n are the thermal conductivity of Si_3N_4 and SiO_2, respectively.

S_c is the shape factor that account for the impact of the shape of test beam on heat conduction to the substrate. The shape factor for heat conduction is given by reference [21].

$$S_c = h/w(2g_{air}/h+1)+1 \quad \text{(B-6)}$$

Where w and h is the width and thickness of test beams, respectively.

(4) The heat convection through the air is

$$Q_{convection} = -h_c(T-T_\infty) \quad \text{(B-7)}$$

Where h_c is the heat convection coefficient.

(5) The heat radiated from the heated test structure with the power source to the air can be approximated to be

$$Q_{radiation,\ air} = -\varepsilon\,\sigma\,(T^4-T_\infty^4) \quad \text{(B-8)}$$

Where ε is the effective absorptivity (or emissivity) of test film, and σ denotes the Stefan-Boltzmann constant.

(6) The heat radiated from the heated test structure with the power source to the substrate is approximated to be

$$Q_{radiation,\ sub} = -wLS_r\,\varepsilon\,\sigma\,(T^4-Ts^4) \quad \text{(B-9)}$$

Where S_r is the radiation shape factor that is given by reference [24].

$$S_r = 2/(\pi AB)\{L_n\sqrt{(1+A^2)(1+B^2)/(1+A^2+B^2)}+A\sqrt{(1+B^2)}\tan^{-1}[A/\sqrt{(1+B^2)}] + B\sqrt{(1+A^2)}\tan^{-1}[B/\sqrt{(1+A^2)}] - A\tan^{-1}[A] - B\tan^{-1}[B]\}$$

Where $A=w/g_{air}$, and $B=L/g_{air}$

For a numerical estimate, we consider the given sample as follow. L=600um, w=3um, h=2um, g_{air}=3um, Ts=T_∞=20℃=293.2k, T=400℃=673.2k, κ_{air}=0.026W/mk, κ_{poly}=14 ~ 41W/mk, h_c=25 ~ 250W/m^{2}k, σ=5.67E-8W/m^{2}k^4, η=1, Λ=1.663E-1Wm^{-2}K^{-1}mTorr^{-1}, P=760mTorr, and ε=0.6 for the polysilicon. Thus,

$Q_{conduction,\ polysi}$= (-41~-14)/600E-6 • (673.2-293.2)= -25966667 W/m^2~ -8866667 W/m^2

$Q_{conduction,\ air}$=-1/4 • 1 • 1.663E-1 • 760 • (273.2/293.2)$^{1/2}$ • (673.2-239.2)= -11589.8 W/m^2

$Q_{conduction,\ air,\ sub}$= -11/3 • 0.026/3E-6 • (673.2-293.2)= -12075558W/ m^2

$Q_{convection}$=-250 • (673.2-239.2)= -95000 W/ m^2

$Q_{radiation,\ air}$ =-0.6 • 5.67E-8 • (400^4-20^4)= -860 W/ m^2

$Q_{radiation,\ sub}$=-3E-6 • 600E-6 • 0.41 • 0.6 • 5.67E-8 • (400^4-20^4)≒0.000… W/ m^2

REFERENCES

[1] W. Riethmuller and W. Benecke. Thermally excited silicon microactuators, IEEE Trans. Electron Devices, vol. 35, (1988) 758-762

[2] H. Matoba, T. Ishikawa, C. J. Kim and R. S. Muller, A bistable snapping microactuator, in Proc. IEEE Workshop, Jan. (1994) 45-50

[3] L. Lin and S. H. Lin, Vertically driven microactuators by electrothermal buckling effects, Sensors and Actuators, vol. A71, (1998) 35-39

[4] T. Lisec, S. Hoerschelmann, H. J. Quenzer, B. Wagner and W. Benecke, Thermally driven microvalve with buckling behavior for pneumatic applications, in Proc. IEEE Workshop, Jan. (1994) 13-17

[5] H. Guckel, J. Klein, T. Christenson, K. Skrobis, M. Landon and E. G. Lovell, Thermo-magnetic metal flexure actuators, Technical Digest, IEEE Solid State Sensor and Actuator Workshop, Hilton Head Island, (1992) 73-75

[6] C. S. Pan and Wensyang Hsu, "An Electro-thermally Driven Polysilicon Microactuator", J. Micromech. Microeng., Vol. 7, (1997) 7-13,.

[7] Comtois, J. J. and Bright, V. M., "Applications for Surface-micromachined Polysilicon Thermal Actuators and Arrays," Sensors and Actuators A 58 (1997) 19-25.

[8] H. Baltes, O. Paul, O. Brand, Micromachined, thermally-based CMOS microsensors, in: Proc. IEEE 86 (1998) 1660-1678.

[9] J. Schieferdecker, R. Quad, E. Holzenkampfer and M. Schulze, Infrared thermopile sensors with high sensitivity and very low temperature coefficient, Sensors and Actuators, A46-47 (1995) 422-427.

[10] F. Volklein, H. Baltes, A Microstructure for Measurement of Thermal Conductivity of Polysilicon Thin Films, J. Microelectromechanical Systems 1 4 (1992) 193-196

[11] V. A. Martin, O. Paul, H. Baltes, Process-dependent thin-film thermal conductivities for thermal CMOS MEMS, J. Microelectromechanical Systems 19 1 (2000) 136-145.

[12] Fedder, G. K. and Howe, R. T., "Thermal Assembly of Polysilicon Microstructures," Proc. IEEE Micro Electro Mechanical System Workshop (1991) 63-68

[13] Y. Fukuta, T. Akiyama and H. Fujta, A reshaping technology with Joul heat for three dimensional silicon structures, the 8th international Conference on Solid State Sensor and Actuator, Sweden, (1995) 174-177

[14] N. S. Mitrovic, S. R. Djukic, S. B. Djuric, Crystallization of the Fe-Cu-M-Si-B (M=Nb, V) amorphous alloys by direct-current joule heating, IEEE Trans. on Magnetics, Vol. 36, No. 5, (2000), 3858-3862.

[15] Y. C. Tai, C. H. Mastrangelo, R. S. Muller, Thermal Conductivity of Heavily Doped Low-Pressure Chemical Vapor Deposited Polycrystalline Silicon Films, J. Appl. Phys. 63 (5) 1 (1988) 1441-1447.

[16] C. H. Mastrangelo, R. S. Muller, Thermal diffusivity of heavily doped low pressure chemical vapor deposited polycrystalline silicon films, Sensors and Materials 3 (1988) 133-142.

[17] M. von Arx, O. Paul, H. Baltes, Test structures to measure the seebeck coefficient of CMOS IC polysilicon, IEEE Trans. on Semiconductor Manufacturing, Vol. 10, No. 2, (1997) 201-208.

[18] C. S. Pan and Hsu W "A Microstructure for in-situ Determination of Residual Strain", IEEE J. Microelectromechanical Systems Vol.8, No.2, (1999) 200-207.

[19] C. S. Pan, "A Simple Method for Determining Linear Thermal Expansion Coefficients of Thin Films", J. Micromech. and Microeng., 12, (2002) 1-8

[20] Chae J H, Lee J Y, and Kang S W "Measurement of thermal expansion coefficient of poly-Si using microgauge sensors", Sensors and Actuators A 75 (1999) 222-229.

[21] L. Lin, M. Chiao, Electrothermal Responses of Line Shape Microstructures, Sensors and Actuators A55 (1996) 31-41

[22] Q-A Huang, N K S Lee, "Analysis and Design of Polysilicon Thermal Flexure Actuator," J. Micromech. Microeng. **9** (1999) 64-70.

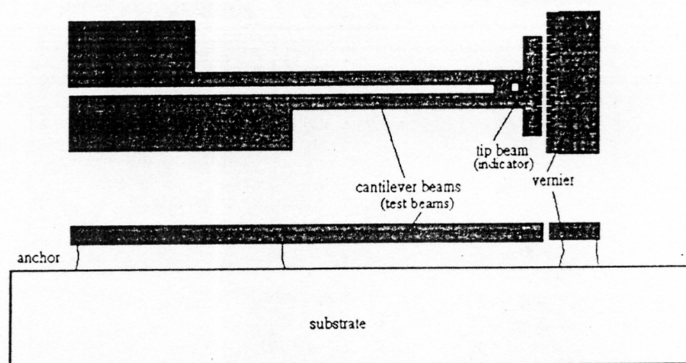

Fig. 1.

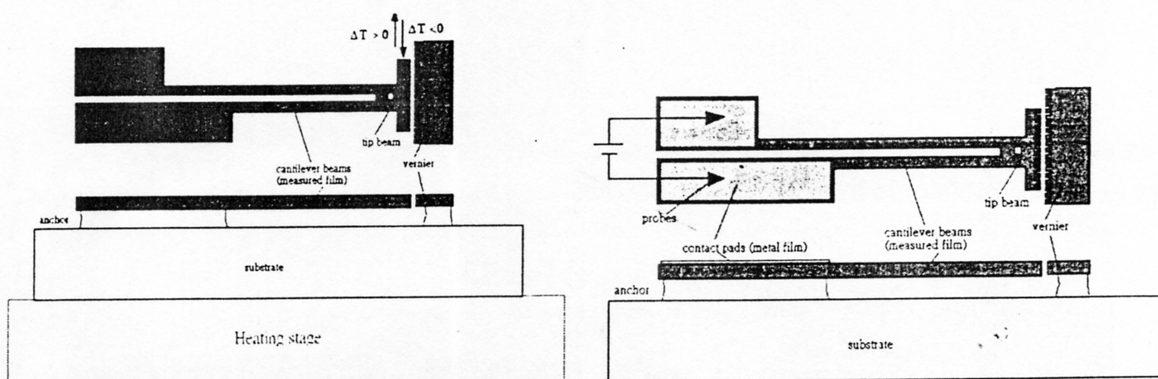

Fig. 2

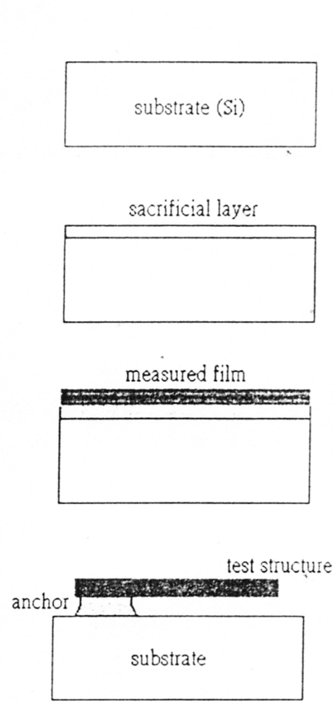

Fig.3

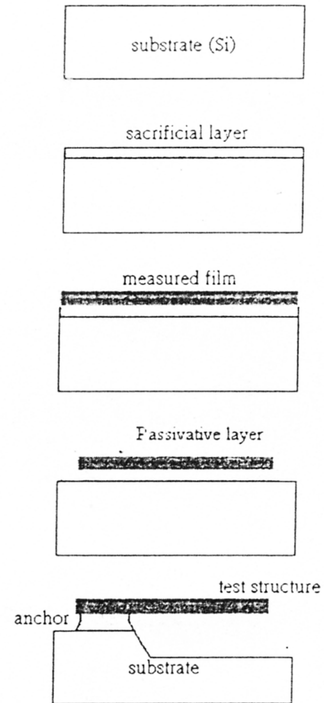

Fig. 4

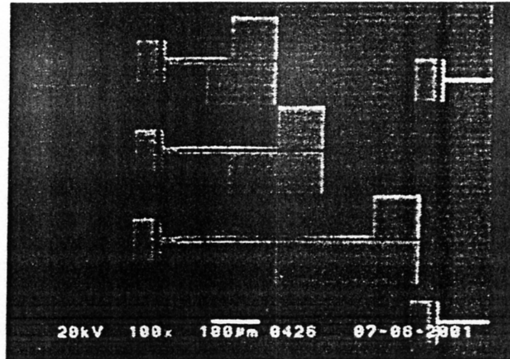

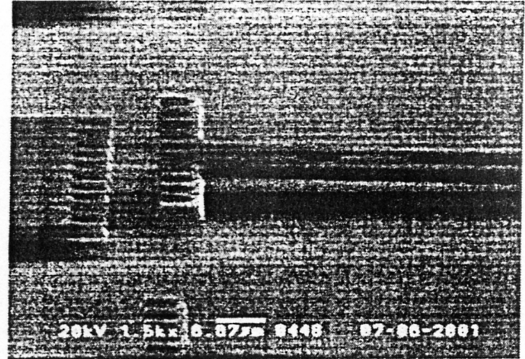

(a)

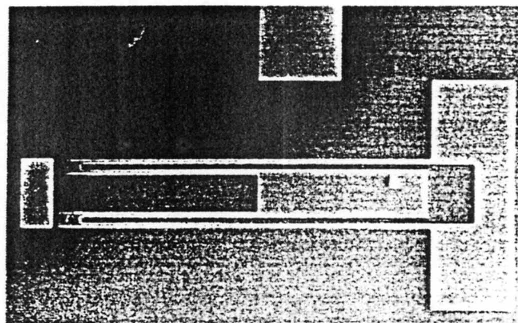

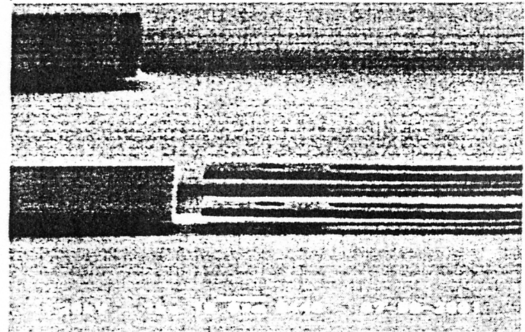

(b)

Fig. 5

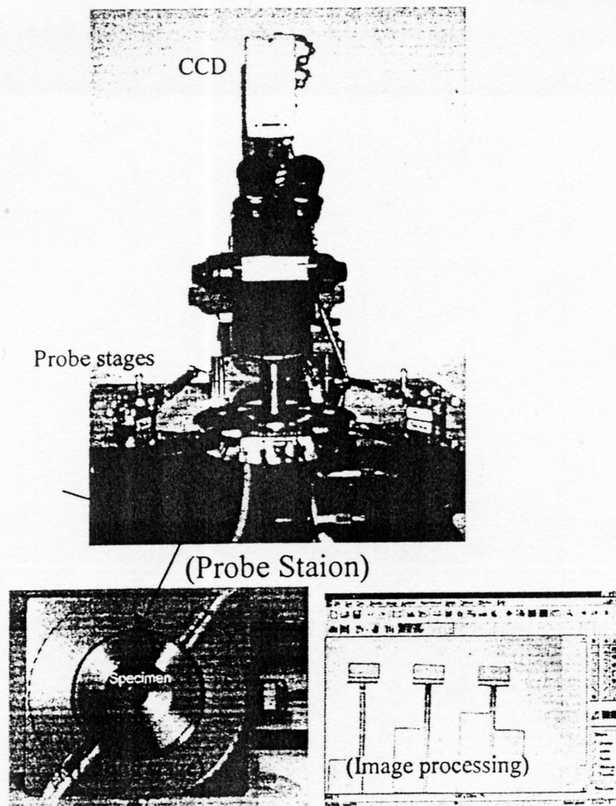

Figure 6.

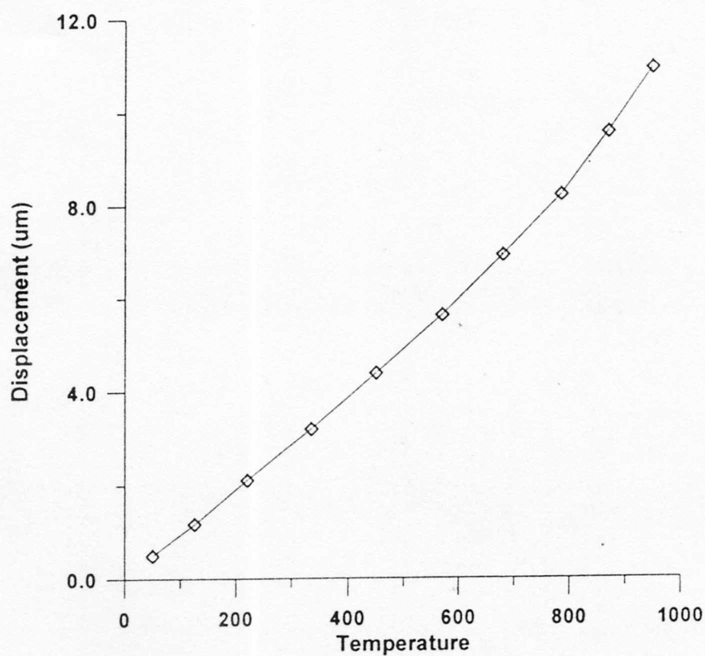

Fig. 7

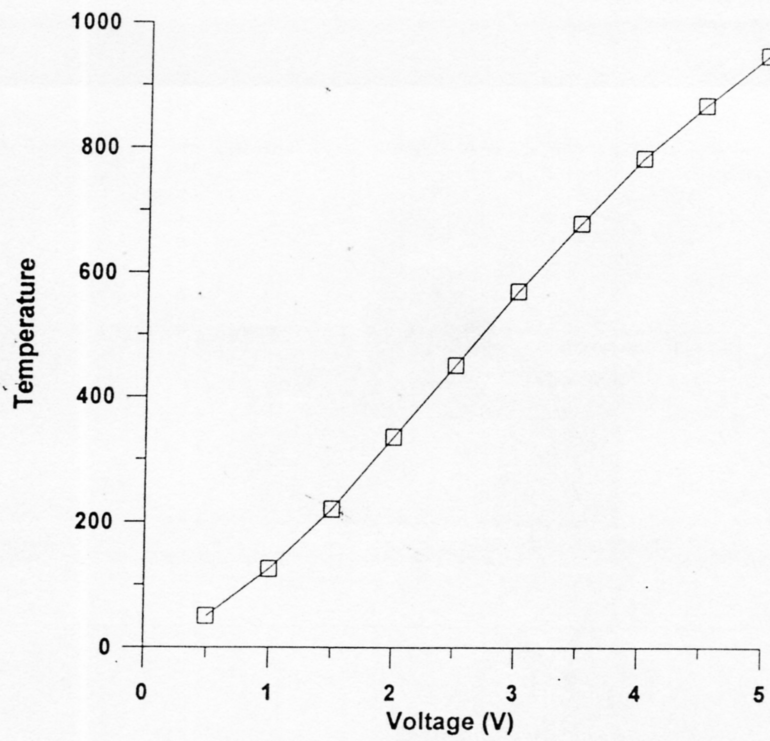

Fig. 8

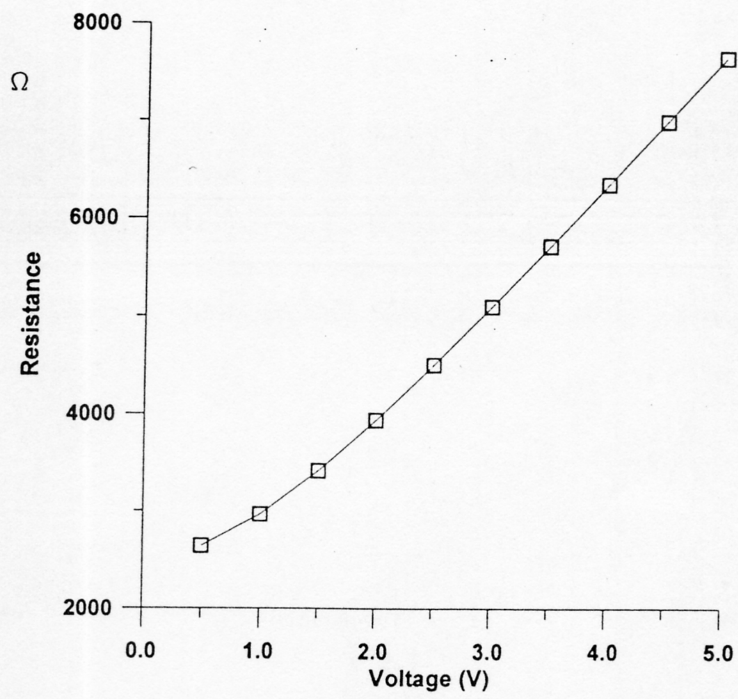

Fig. 9

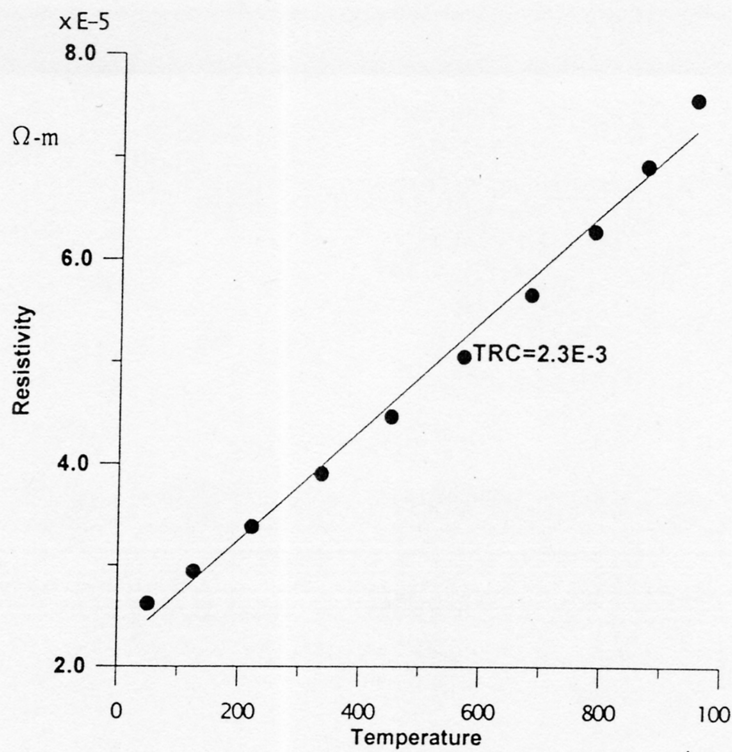

Fig. 10